RSC Advances

RSC Advances

www.rsc.org/advances

ROYAL SOCIETY OF CHEMISTRY

www.rsc.org/advances

Hollow Au-Ag Bimetallic Nanoparticles with High Photothermal Stability

R. C. Carrillo-Torres[1*], M. J. García-Soto[2], S. D. Morales-Chávez[3], A. Garibay-Escobar[3],

J. Hernández-Paredes[1], R. Guzmán[2], M. Barboza-Flores[4], M. E. Álvarez-Ramos[1]

[1] Departamento de Física, Universidad de Sonora, Blvd. Luis Encinas y Rosales sn. Col. Centro, Hermosillo, Sonora 83000, México.

[2] Department of Chemical and Environmental Engineering, The University of Arizona, 1133 E James E. Rogers Way, Tucson, AZ 85721, USA.

[3] Departamento de Ciencias Químico Biológicas, División de Ciencias Biológicas y de la Salud, Universidad de Sonora, Blvd. Luis Encinas y Rosales sn. Col. Centro, Hermosillo, Sonora 83000, México.

[4] Departamento de Investigación en Física, Universidad de Sonora, Apdo. Postal 5-088, Hermosillo, Sonora 83190, México.

ABSTRACT

Noble metal nanoparticles have received much attention due to their interesting properties that make them useful in different technical fields. Metallic nanoparticles with optical properties in the near infrared region of the electromagnetic spectrum are of great importance for biological applications, in particular photothermal therapy, as it is greatly enhanced by metallic nanoparticles. However, despite the large amount of work that has been done with metallic nanoparticles for thermal therapy, there is a reduced amount of scientific reports about the photothermal stability of most studied nanoparticles. In this work, hollow Au-Ag bimetallic nanoparticles were synthesized *via* galvanic replacement reaction, with optical properties that can be tuned systematically along the visible and near infrared region of the spectrum, by changing the pH before the synthesis of the templates and by controlling the amount of gold added for the synthesis of the nanoshells. The synthesized nanoparticles exhibit good photothermal properties when illuminated with an 808 nm laser light. An increase of temperature of nearly 20 °C is achieved after 15 minutes of irradiation. Moreover, the Au-Ag nanoparticles show good reusability even after ten heating/cooling cycles. The nanoparticles also retain their optical properties after 12 hours

---

[*] Corresponding author. Tel. +52 (662) 259-2108
e-Mail address: rn_carrillo@hotmail.com

of continuous irradiation and are able to maintain their photothermal characteristics of increasing the temperature at the same levels during the entire process.

INTRODUCTION

In the last decade, noble metal nanoparticles (NPs) have received much attention due to their interesting properties that make them useful in photonics,[1] catalysis,[2] and biomedical applications.[3] Particularly, the optical properties are of great importance for biological applications.

The optical properties of metallic NPs are due to their interaction with the electromagnetic field of light, which induces a collective coherent oscillation of the free electrons on metals. This process is resonant at specific wavelengths and it is called localized surface plasmon resonance (SPR).[4] The optical properties of metallic NPs can be tuned to absorb light of different wavelengths by controlling some parameters such as: size, shape, structure, and shape factor.[5]

For biological applications, it is desirable to use near infrared (NIR) electromagnetic radiation, specifically, wavelengths located in the biological window (650-900 nm), because of the high transparency of soft tissues, blood, and water in this wavelength interval.[4] There are at least, three different ways to shift the SPR band of gold nanoparticles to the NIR region: 1) by forming aggregates of spherical NPs, 2) by elongation of the particles into rods, and 3) by producing hollow nanostructures.[6] Hollow gold nanospheres are ideal for thermal ablation because their strong photothermal conversion as a result of the combination of their properties like small size, spherical shape, and SPR tunability in the NIR region.[7]

Particles at the nanoscale are easy to incorporate in biological systems. One example of biomedical application is photothermal therapy, which is greatly enhanced by metallic NPs. This therapy can operate in three basic modes: light only, light with organic dyes for photothermal conversion, and light with metal nanoparticles, being the last one more effective in terms of heat generation due to the more efficient photothermal conversion of metals.[8]

Despite the large amount of work that has been done with metallic nanoparticles for thermal therapy, there is a reduced amount of scientific reports about photothermal stability of nanoparticles under long exposure times to continuous wave (CW) laser light or under several heating/cooling cycles. Thermal stability is an important aspect for metallic nanostructures because the reduced melting temperatures observed at the nanoscale can affect their structural integrity and morphology and consequently their optical properties when heated.[9]

Recently, Fu *et al.* reported the decrease in the photothermal efficiency of gold nanorods after only four heating/cooling cycles under a 808 nm laser light during 10 minutes of operation.[10] Similar results were obtained by Tian *et al.,* when comparing the photothermal properties of Fe_3O_4/CuS nanoparticles with gold nanorods after six repeated heating/cooling cycles upon excitation with a 980 nm laser.[11] In such study, it was observed the decrease of the maximum temperature achieved by the gold nanorods after each cycle. Although there are ways to improve the thermal stability of nanoparticles, the procedures require additional synthetic steps, for example capping the nanoparticles with a thin layer of silica or polymer is among the proposed strategies.[12, 13] However, the thermal stability of these systems has only been evaluated for short illumination times, in general within the minute scale.[12, 13]

In this paper, we report the synthesis and characterization of hollow Au-Ag bimetallic nanoparticles with tunable optical properties along the visible and near infrared region of the electromagnetic spectrum obtained by a galvanic replacement reaction. We also report their photothermal properties and thermal stability after ten heating/cooling cycles and after long exposure times to CW laser light.

EXPERIMENTAL

Materials

Silver nitrate ($AgNO_3$, ≥99%), sodium citrate dihydrate ($Na_3C_6H_4O_7·2H_2O$, ≥99%), ascorbic acid ($C_6H_6O_6$, ≥99%), sodium hydroxide (NaOH, ≥98%), hydroxylamine hydrochloride ($NH_2OH·HCl$, ≥99%) and tetrachloroauric (III) acid ($HAuCl_4·3H_2O$, ≥99.9%) were purchased from Sigma-Aldrich Co. (St. Louis, MO). All the glassware was

washed with soap, aqua regia, and rinsed several times with tap water and deionized water. Ultrapure water with a resistivity of 18.2 MΩ·cm was used in all experiments.

Synthesis of silver templates

Synthesis of silver templates was carried out using ascorbic acid as reductant and sodium citrate as stabilizer as reported from Qin *et al.*[14] In a typical experiment, 10 mL of aqueous solutions containing ascorbic acid (0.6 mM) and sodium citrate (3 mM) were adjusted to different pH values (8.0, 9.0, 10.0 and 10.5) using a 0.5 M sodium hydroxide solution. Next, the temperature of the solution was increased to 30 °C in a water bath, followed by the addition of 0.1 mL of a 0.1 M silver nitrate solution under vigorous stirring during 30 minutes. Once the reaction time elapsed, the temperature was increased to 80 °C for 2 hours. Finally, the reaction was left to cool at room temperature.

Synthesis of hollow nanoparticles

Hollow nanoparticles were prepared by reducing tetrachloroauric acid onto silver templates. First, the entire volume of silver templates was diluted to 50 mL followed by the addition of 1 mL of a 0.1 M hydroxylamine hydrochloride solution. After mixing during 5 minutes, aliquots of 10 mL from each stock were heated in a water bath at 60 °C. Once the reaction mixture reached the mentioned temperature, hollow nanoparticles were synthesized by adding different volumes (20-100 μL) of a 25 mM tetrachloroauric acid solution to the silver templates under vigorous stirring and were left to react for 30 minutes. The color of the suspension changed immediately from yellow to violet, blue, blue green or greyish green depending on the volume of gold added. The obtained hollow nanoparticles were left to reach room temperature and stored.

Characterization

The extinction spectra of colloidal solutions were obtained with an Ocean Optics USB2000+XR1-ES spectrometer. The particle size was determined by dynamic light scattering (DLS) using a Malvern Zetasizer Nano ZS equipped with a He-Ne laser (λ = 632.8 nm). Water-dispersed nanoparticles were deposited on 400-mesh carbon-coated copper grids and transmission electron microscopy (TEM) images were obtained with a

JEOL 2010F operating at 200 kV. STEM images were obtained with a Hitachi STEM-5500 equipped with a solid-state Bruker Nano detector operating at 30 kV.

Heating Experiments

The heating experiments were carried out using a volume of 1.5 mL of hollow nanoparticles in a quartz cuvette with samples adjusted to different optical densities. A type K thermocouple connected to a digital thermometer Reed SD-947 (Reed Instruments, Canada) was inserted in the sample through a perforated PTFE cap and sealed with parafilm to prevent evaporation. The samples were illuminated using a CW 808 nm collimated diode laser (Laserglow Technologies, USA) delivering a maximum power output of 1 W over an area of 0.5 cm^2. The heating profiles were obtained by automatic recording the temperature every 10 seconds. The measurement sequence consisted of three stages: an initial recording during 3 minutes to obtain the mean room temperature, followed by an illumination time of 30 minutes until reaching a steady value, and a final cooling interval of 10 minutes.

Cell viability assay

The cytotoxicity of the synthesized nanoparticles was evaluated by MTT method. Adenocarcinomic human cell line, A549, was cultured in DMEM medium supplemented with 5% fetal bovine serum, 100 U/mL penicillin and 0.1 mg/mL streptomycin in a humidified incubator at 37°C with 5% CO_2. Cells were detached from culture flask by trypsinization and the cell suspension was adjusted to a concentration 200,000 cells/mL. 50 µL of cell suspension were plated on a 96-well plate and incubated during 24 hours. Then, 50 µL of nanoparticle solution (previously diluted in culture medium and adjusted to different optical densities) were added; every concentration was evaluated by triplicate. The plate was incubated during 48 hours. Afterwards, the culture medium was eliminated and the cells were washed with PBS followed by the addition of 100 µL of culture medium and 10 µL of MTT, the plate was incubated during 4 hours. Finally, 100 µL of acidic isopropanol were added to resuspend formazan crystals and absorbances were read at 570 and 630 nm wavelengths in a microplate reader. Cells not exposed to nanoparticles were

used as control. The results of the experiments were expressed as percentage of cell viability.

RESULTS AND DISCUSSION

Synthesis of silver templates

Stable suspensions of silver nanoparticles with different sizes were synthesized at different pH values. Figure 1 shows their normalized extinction spectra with absorption peaks located at 423, 420, 415 and 409 nm, for pH values of 8.0, 9.0, 10.0 and 10.5, respectively. This shift to shorter wavelengths as the pH value increases is in good agreement with the average hydrodynamic diameter obtained by DLS of the synthesized templates (Figure 1, inset). In agreement with theory, the surface plasmon resonance band is shifted to longer wavelengths as the size of the nanoparticles increases.[15] The average diameter of the obtained particles decreases at higher pH, a behavior attributed to the different reactivity of ascorbic acid under different pH conditions. At higher pH values, the number of nucleus produced in the early stages of the reaction increases due to a promoted reactivity of ascorbic acid mediating the number of nucleus and therefore the final size of the nanoparticle.[14] In this way, it is possible to easily tune the size of the templates by simply changing the pH of the reaction, allowing the control over the cavity size of the final hollow nanoparticles and their optical properties along the visible and near infrared spectrum.
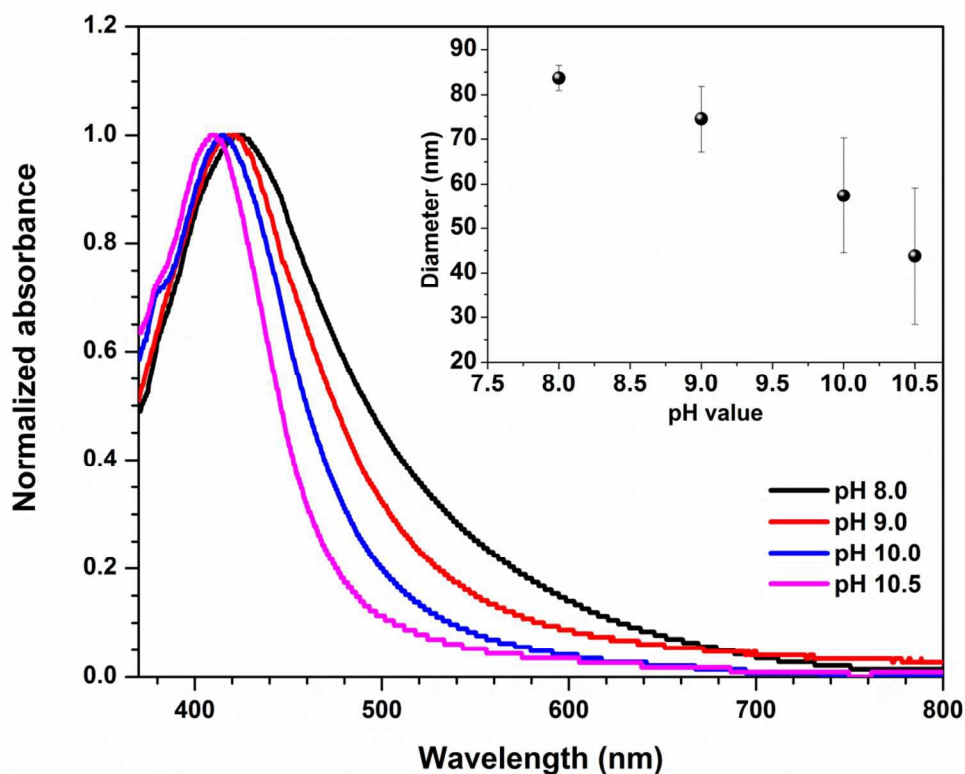
Figure 1. Normalized extinction spectra of silver nanoparticles synthesized at different pH values and its mean size and standard deviation as measured by DLS (inset).

Synthesis of hollow nanoparticles

Hollow nanoparticles were obtained in all reactions by adding tetrachloroauric acid to silver template suspensions. The typical growth mechanism for the shell is a redox reaction involving the reduction of ionic gold onto the surface of the silver template *via* galvanic replacement. At the same time that the ionic gold on the surface is reduced into metallic gold, silver is oxidized into ionic silver according to the following reaction:

$$3Ag_{(s)} + [AuCl_4]^{-1}{}_{(aq)} \rightarrow Au_{(s)} + 3Ag^{+1}{}_{(aq)} + 4Cl^{-1}{}_{(aq)} \qquad (1)$$
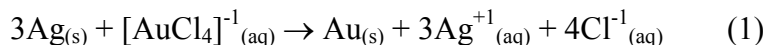
Silver is oxidized due to its lower reduction potential (Ag^{+1}/Ag 0.8V, versus standard hydrogen electrode (SHE)) compared to that of gold ($AuCl_4^{-1}$/Au 0.99V, versus SHE), displacing 3 silver atoms from the template for every gold atom deposited on its

surface.[16,17] The reaction occurs through the pinhole dissolution of the core involving an alloying/dealloying process, with the epitaxial deposition of gold on the surface of each template due to the good matching between the crystalline structure and lattice constants of gold and silver, 4.0786 and 4.0862 Å, respectively). In the final stage of the reaction, ionic silver reacts with the chlorine ions producing silver chloride powder as by-product.[18] However, the galvanic process can be modified under specific conditions, affecting the growth mechanism and the composition of the final structure.[19]

Figure 2 shows the normalized extinction spectra of the hollow nanoparticles obtained after the addition of different amounts of tetrachloroauric acid. The spectra gradually red-shifts with the increase of the gold concentration, reaching a maximum at 0.20 mM, followed by a blue shift at higher concentrations. This effect is consistent with the nucleation and growth of the shell around the dissolving template; in a later stage, thickening the shell and blue-shifting its extinction spectra.[20, 21]
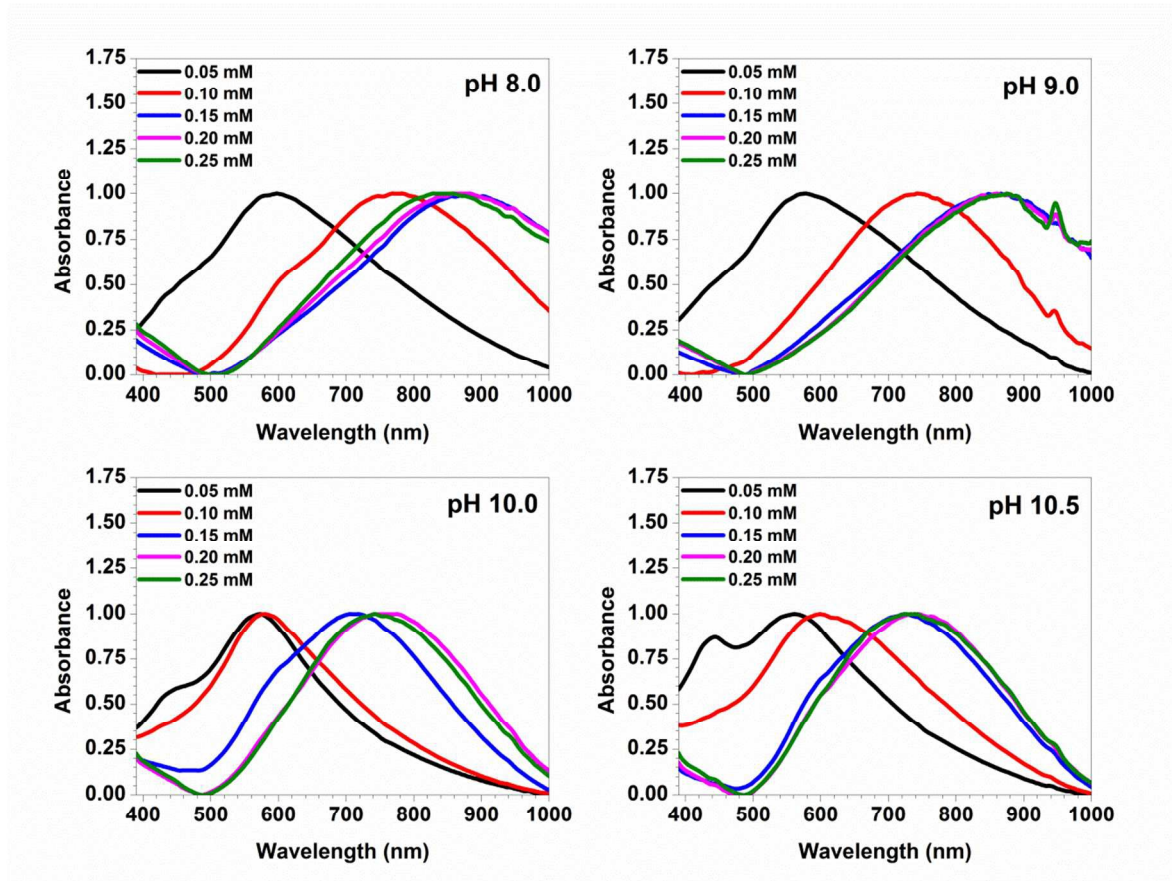
Figure 2. Extinction spectra of hollow nanoparticles obtained after different amounts of gold were added to silver templates synthesized at different pH values.

The synthesized nanoparticles can be readily tuned to absorb light along the visible and near infrared part of the electromagnetic spectrum by adjusting the template size and the concentration of gold. The spectra of the obtained hollow nanoparticles are characterized by broad bands of several hundred nanometers, due to the different characteristics of the sample. In the micrographies from a sample prepared at pH 8.0 it is possible to see a large distribution of spheroidal nanoparticles and a lesser amount of distorted hexagons, fused nanoparticles and rod-like particles, all with different shell thicknesses and hollow cores (Figures 3A and 3B). These results would suggest that further control over the reaction is needed to improve the size distribution and the shell thickness. As mentioned before, the shape of the absorption band depends not only on the size of the particle, but also on the geometry and thickness of the shell, [5] thus contributing to the broadening of the extinction spectra. In Figure 3C it is possible to observe the

polycrystalline nature of the nanoparticle, some interplanar spacings corresponding to {111} family are indicated.
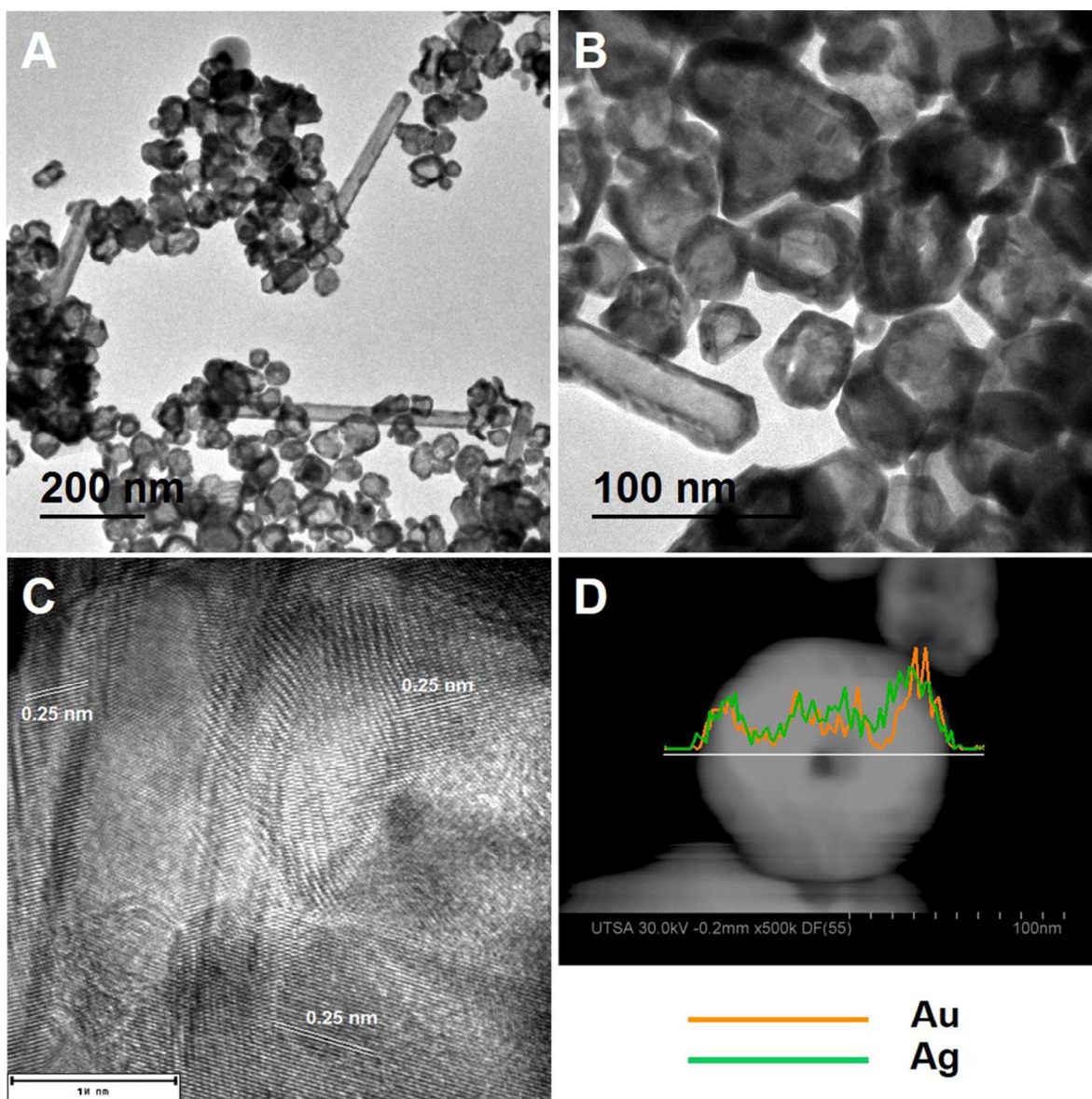
Figure 3. Transmission electron micrographies from a sample prepared at pH 8.0 and Au/Ag molar ratio 1.0 at different magnifications (A, B); HRTEM images indicating the {111} interplanar spacing (C); EDS line-scan of an isolated nanoparticle indicating the presence of both metals in the nanostructure (D).

It is worth to mention, that during the synthesis a small production of silver chloride was detected. Furthermore, it is possible to see that the most red-shifted extinction spectra corresponds to an Au/Ag molar ratio near to 1.00 instead of 0.33 as expected from a typical galvanic replacement reaction (Figure 4), thus indicating a different growth mechanism.
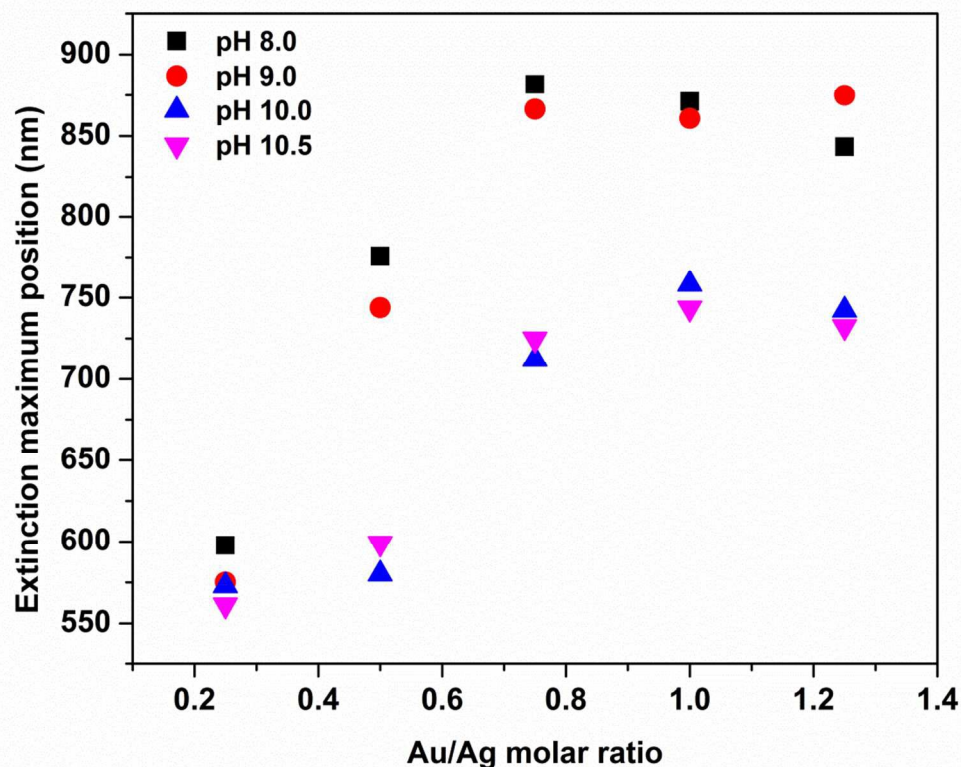
Figure 4. Position of the maximum extinction of the hollow nanoparticles as function of the Au/Ag molar ratio.

It has been reported that the galvanic replacement can be prevented or modified in presence of hydroxylamine and sodium hydroxide, [22] since the reducing power of the former is enhanced at high pH.[17] It can also be inhibited when ascorbic acid is paired with sodium hydroxide.[23, 24] All the compounds mentioned above are present in low concentrations in our system, except for hydroxylamine. In the presence of a mild reductant, the silver templates act as mediators of electron transfer to catalyze the reduction of ionic gold on the chemically oxidized ionic silver while being deposited on its surface,[17, 22] where the following reactions occurs:

$$(Ag_n)_{(s)} + [AuCl_4]^-_{(aq)} \rightarrow (Ag_nAu)_{(s)} + 4Cl^- \qquad (2)$$

$$(Ag_nAu_m)_{(s)} + [AuCl_4]^-_{(aq)} \rightarrow (Ag_nAu_{m+1})_{(s)} + 4Cl^- \qquad (3)$$

$$(Ag_nAu_m)_{(s)} + Ag^+_{(aq)} \rightarrow (Ag_{n+1}Au)_{(s)} \qquad (4)$$
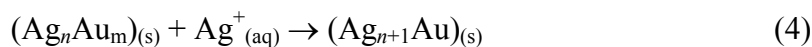
Furthermore, at earlier stages of the reaction, hydroxylamine can change the oxidation state of gold ions from trivalent to monovalent form during the initial gold coating of the template modifying the replacement reaction pathway.[22] During the initial stage, a thin and incomplete layer of gold is deposited on the surface of the template, preventing the oxidation of the silver core. Next, the pinholes on the newly gold deposit serve as active sites to start the dissolution of the template.[16] In the presence of $[AuCl_2]^-$, the pinholes disappear with the addition of a small amount of precursor. In contrast, when $[AuCl_4]^-$ is used, the pinholes remain open until much more precursor is added. The early disappearance of pinholes for the reaction with monovalent gold is attributed to a 1:1 molar ratio obtained between the generated Au and the consumed Ag, resulting, in consequence, that a greater volume of precursor solution is required in this case than when $[AuCl_4]^-$ is used. Since there is no pinhole for the reaction species to diffuse in and out from the former system, silver must diffuse through the gold layer in order to be oxidized and dissolved, producing a homogeneous Au/Ag alloy, which is more thermodynamically stable than either pure Au or Ag.[16, 25, 26] Moreover, this change in oxidation state of gold also influences the final composition and thickness of the shell.[25]

In the present work, the final composition of the hollow nanoparticles has a bimetallic character as was confirmed by energy dispersive spectroscopy (EDS). Figure 3D shows a line-scan over an isolated nanoparticle, which clearly indicates the coexistence of both metals in the nanostructure. Further, Figure 5 displays the EDS mapping of the sample prepared at pH 8.0 using an Au/Ag molar ratio of 1.0, confirming that the dealloying process in the later stage of galvanic reaction cannot be completed. Figure ESI2 shows the general EDS spectrum of the same sample, which has a composition of 51.49 wt. % Au, 37.46 wt. % Ag and 4.04 wt. % Cl. The presence of chlorine could be attributed to the production of silver chloride, as by-product.
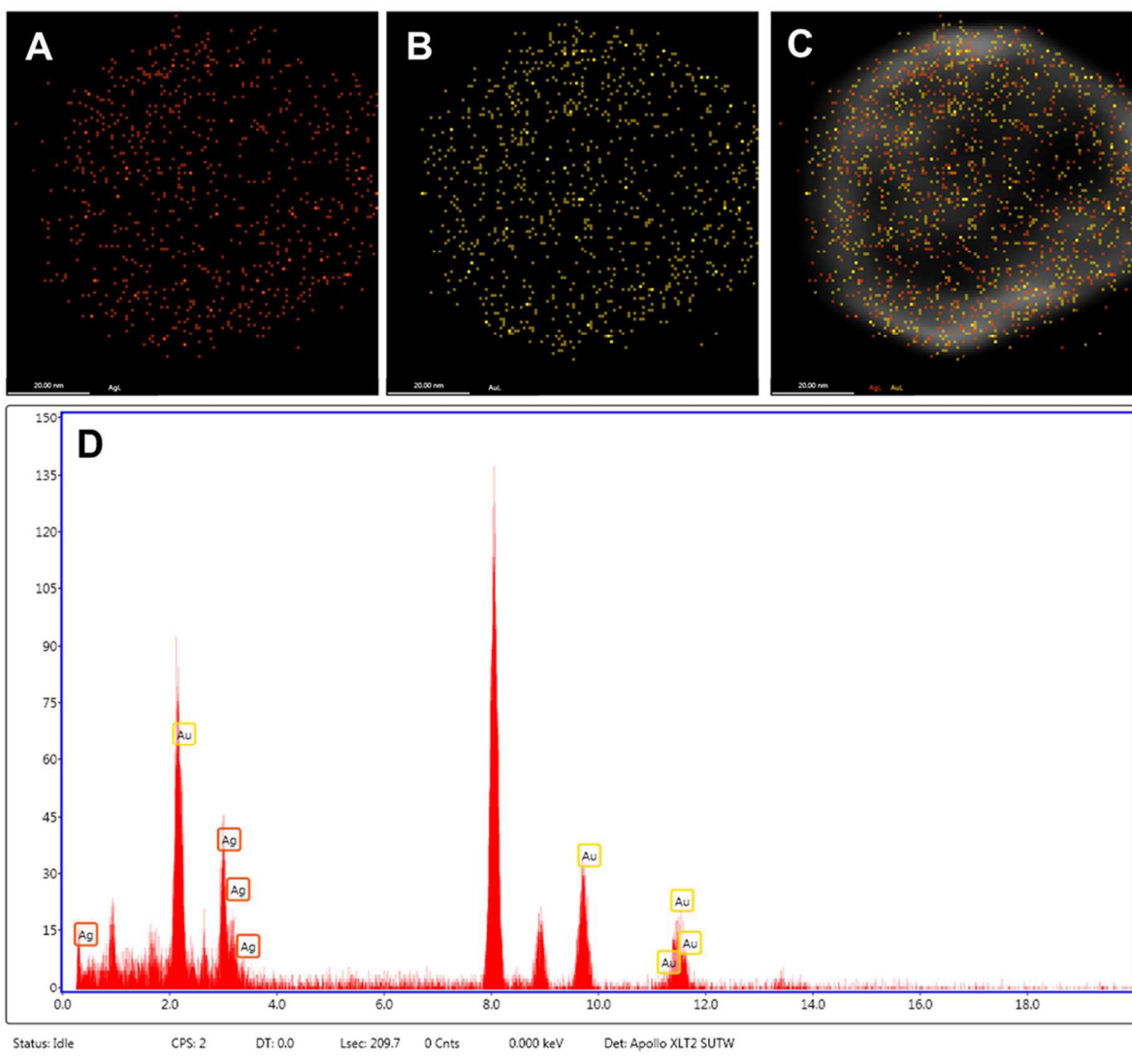
Figure 5. EDS mapping of an isolated hollow nanoparticle synthesized at pH 8.0 and Au/Ag molar ratio of 1.0. Distribution of silver (A) and gold (B) atoms, and the overlay of the two elements (C). The EDS spectrum of the particle indicate the coexistence of gold (yellow squares) and silver (orange squares) in the nanostructure (D).

Heating experiments

Figure 6A shows the thermal behavior of aqueous solutions containing hollow nanoparticles (synthesized at pH 8.0, with final gold concentration of 0.20 mM), adjusted to different optical densities and illuminated with a NIR laser with emitting light at a wavelength of 808 nm. The four stages of the measurement are clearly seen. During the initial phase with the laser off, the NPs are in thermal equilibrium with their surroundings followed by an increase in temperature when the laser is turned on. Then, a steady state temperature is achieved after about 15 minutes, with a temperature increase of nearly 20

°C, which remained constant during the rest of the illumination. It is important to mention that the thermocouple was located near 1 cm above the laser spot at all times during the experiment to avoid interaction with the laser beam. The maximum temperature achieved in this photothermal process is related to the ability to convert photons into heat and this capability depends on the absorption efficiency of the nanoparticle.[27] Finally, when the laser was turned off the samples immediately experienced an exponential cooling process from the final reached temperature to the initial room temperature. Our results are comparable with those reported by other groups under similar conditions.[27-30] Additionally, we have studied the power dependence of the heating properties of the hollow nanoparticles. The experiment was carried out using a nanoparticle solution adjusted to 1.0 absorbance units and illuminated with the same light source while varying the laser power (Figure 6B). The laser power was varied using absorptive neutral density filters. From the graphs it is possible to see that the maximum temperature achieved can be adjusted varying the nanoparticle concentration as well as the power of the incident laser, allowing a fine tuning of the heating properties.
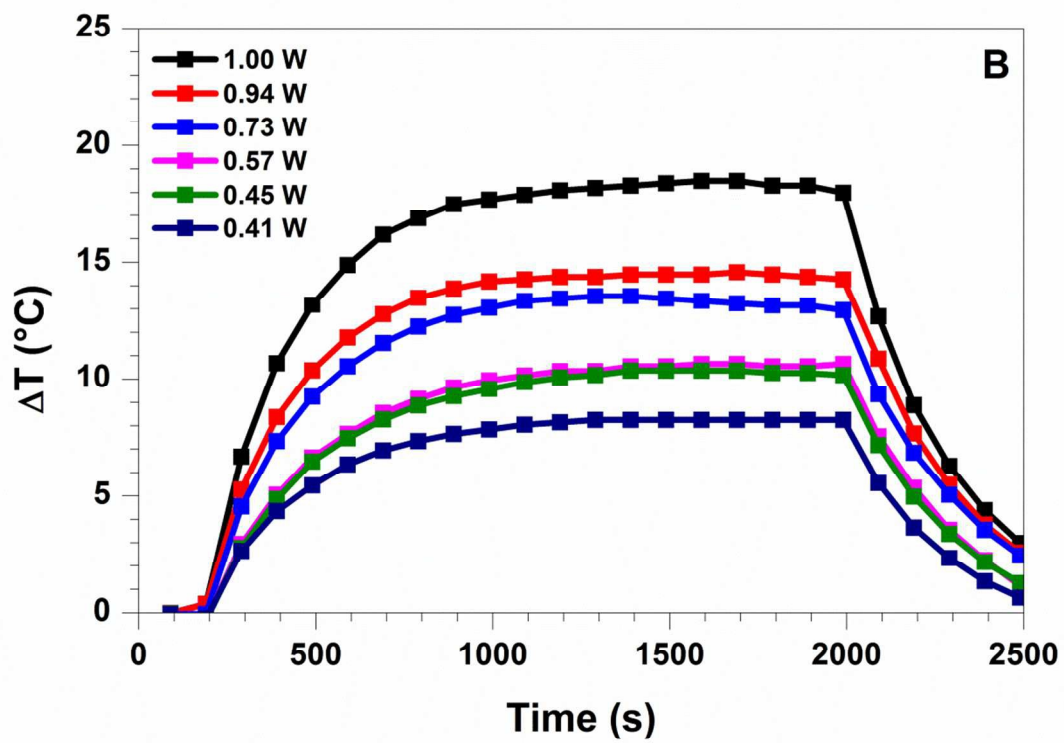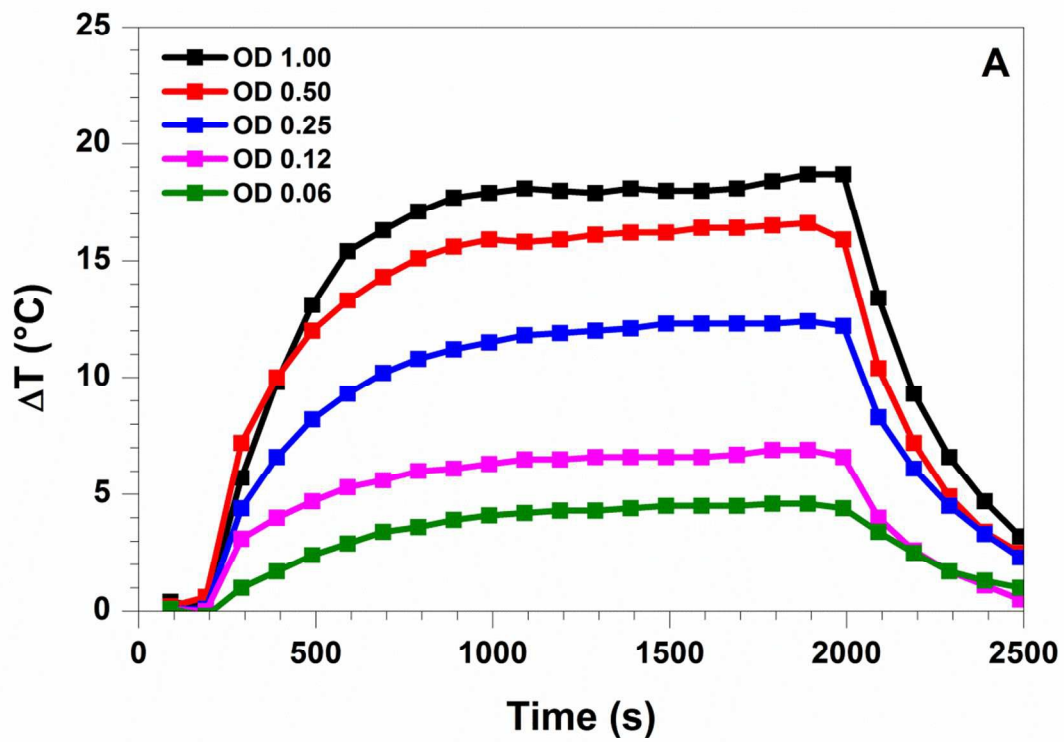
Figure 6. Calorimetric data showing the heating profile due to irradiation with 808 nm laser light of hollow nanoparticles solutions adjusted to different optical densities (A). Heating profile of a nanoparticle solution adjusted to 1.0 absorbance units illuminated with 808 nm light varying laser power (B).

The photothermal transduction efficiency (η) was calculated according to the energy balance reported by Roper *et al*.[31] The energy output was calculated by fitting the cooling portion of the curve after the laser was turned off (See Electronic Supplementary Information and Figure ESI3). The calculated η value was 74.68%, which is slightly superior respect other systems,[32, 33] and comparable with the results obtained by Liu *et al*. using hollow bimetallic urchin-like nanoparticles,[34] but far below gold nanorods.[35]

With nanoshells, as it happens to all optical materials, an important issue is the thermal stability of the system. Melting temperatures significantly lower than that of the bulk material are characteristic of metallic nanostructures. A depressed melting temperature could affect their structure, morphology, and thus the optical properties of the nanostructure when heated.[9] Furthermore, there are reports on the instability of metallic nanoparticles under CW laser irradiation after a few heating/cooling cycles or under short illumination times, diminishing their heating properties.[10-13]

An important feature found in the synthesized particles (pH 8.0, 0.20 mM gold concentration) was their good photothermal stability. The produced NPs in these experiments displayed minimal variation between the maximum temperatures achieved after several heating/cooling cycles. These findings may have important implications for photothermal ablation therapy because it offers the possibility to use lower amounts of NPs injected in the body. In other words, the particles can be reutilized during the therapy process without the necessity to add additional amounts of NPs to the targeted living tissue, minimizing the possible toxicological effects associated with the NPs. In these experiments, the samples were heated up with laser radiation until a final maximum temperature was reached (during 15 minutes as shown in Figure 6) and left to cool down during 10 minutes. This heating/cooling cycle was repeated ten times (Figure 7A). The average temperature gradient reached was around 18 °C with a slight variation (2°C). Furthermore, there was no change in the extinction spectrum of the sample after 10 cycles, suggesting that the synthesized nanoparticles were not damaged, retaining their optical properties (Figure 7C). The latter result is in good agreement with results obtained by other groups after a heating

cycle using a CW laser source in similar structures.[27, 34, 36, 37] The integrity of the samples was confirmed by TEM images of the nanoparticles before (Figure 7B) and after (Figure 7D) the experiments. The nanoparticles displayed minimal changes in their morphology and size distribution.
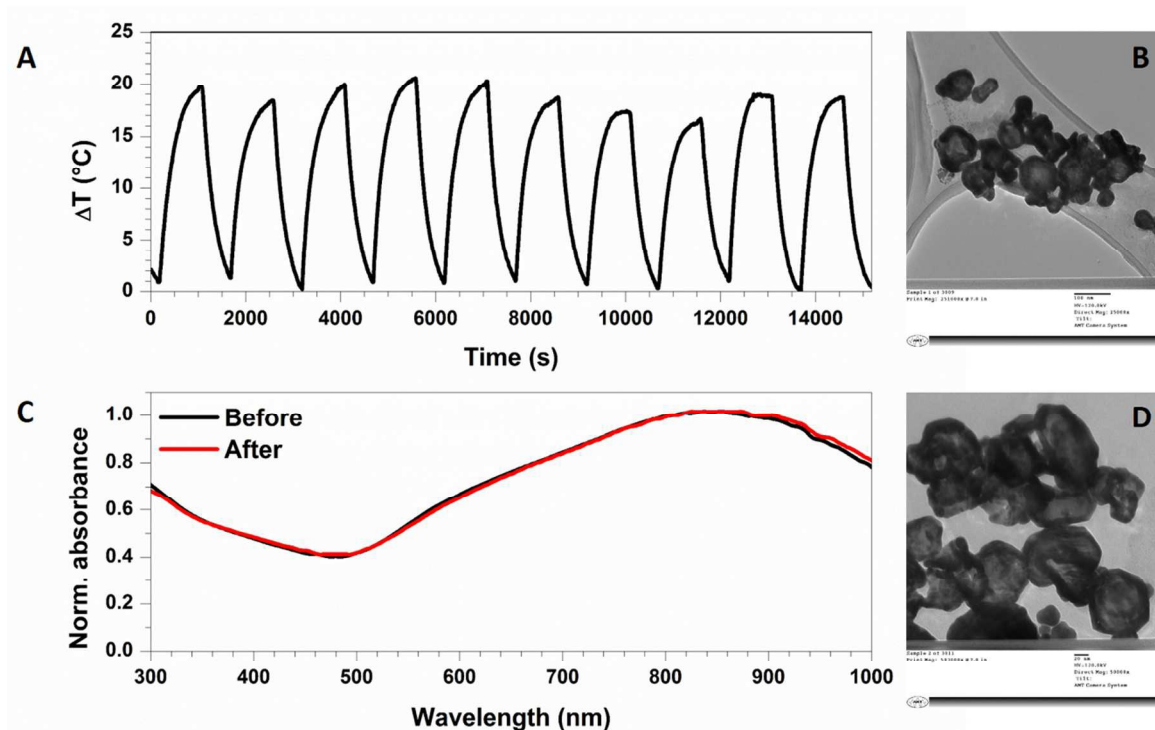
Figure 7. Heating profiles of aqueous solutions of hollow nanoparticles adjusted to 1.0 absorbance units exposed to 10 heating/cooling cycles using 808 nm laser light and its extinction spectra before and after the heating/cooling experiment (A); TEM micrographies of the nanoparticles before (B) and after (C) the heating/cooling experiment.

Additional experiments were carried out to corroborate the stability of the photothermal properties after long irradiation times. A sample of 4 mL was illuminated with laser light of 808 nm in a continuous way during 12 hours. Figure 8 displays that after the first 15 minutes of illumination, the temperature of the sample remained almost constant (25 °C) during the entire illumination time. Another important aspect to note is that the optical properties of the sample remained practically unaltered, with a small blue shift of just 3 nm compared with the initial spectrum (Figure 8A, inset). Besides, according to TEM images, there are no signs of important changes in the morphology of the nanoparticles after the experiment (Figures 8B and 8C, before and after laser exposure, respectively).

This observation would suggest that the NPs are able to retain their morphology for at least 12 hours of irradiation exposure.
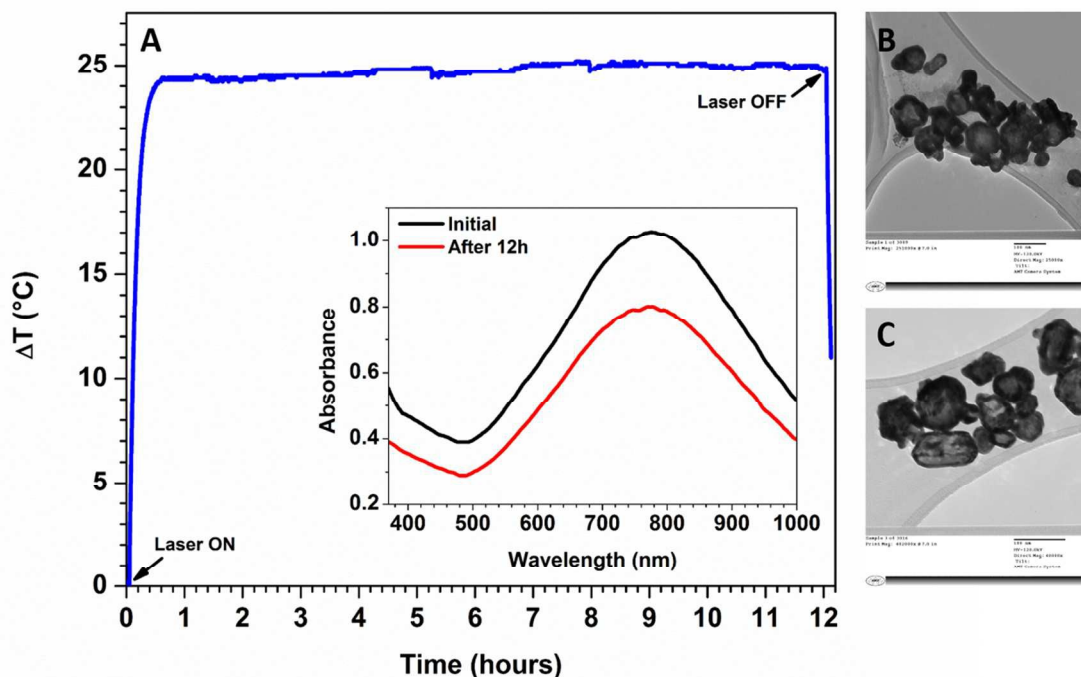
Figure 8. Heating profile of hollow nanoparticles solution adjusted to 1.0 absorbance units irradiated in a continuous way during 12 hours and its extinction spectra before and after the experiment (inset) (A); TEM micrographies of the sample before (B) and after (C) the experiment.

The good heating properties of the synthesized nanoparticles along with their photothermal stability after long illumination periods not only allow their use in biomedical applications, but possibly in many other technical relevant processes where plasmonic nanoheaters could be implemented.

Given the potential applications of the nanoparticles, it is important to evaluate their stability under different pH conditions. For this purpose, solutions of nanoparticles were prepared and adjusted to pH values between 2 and 11 and their extinction spectra were obtained after an incubation period of 15 minutes (Figure ESI5). Between pH 5 and 10, the nanoparticles presented good stability with minimal changes in their extinction spectra. However, at lower pH values the spectra displayed important changes that are more remarkable as the pH value decreases. These changes may be due to the protonation of the

different carboxylate groups in the citrate molecules causing aggregation of the nanoparticles and therefore lower absorptions and red-shifts in the absorption bands. According to this results, it is suggested that the photothermal properties of the nanoparticles are little affected between pH 5 and 10.

Cell Viability Assay

One of the main properties that a nanostructure requires for biomedical applications is a null or low toxicity.[38]. Cytotoxic effects were evaluated by MTT method using A549 cell line exposed to different concentration of hollow nanoparticles; the results are plotted in Figure 9. Due to laboratory limitations the concentration of the sample is expressed in absorbance units. From the graph it is possible to observe that at low optical densities the samples exhibit very low toxicity, with cell viability over 80%, for more concentrated samples cell viability reduces dramatically to values below 10%. Nevertheless, an optical density of the sample with 0.25 absorbance units can achieve an increase in temperature over 10 °C (Figure 6A), which is enough to inhibit the growth and induce cytotoxic effects in mammalian cells.[39]
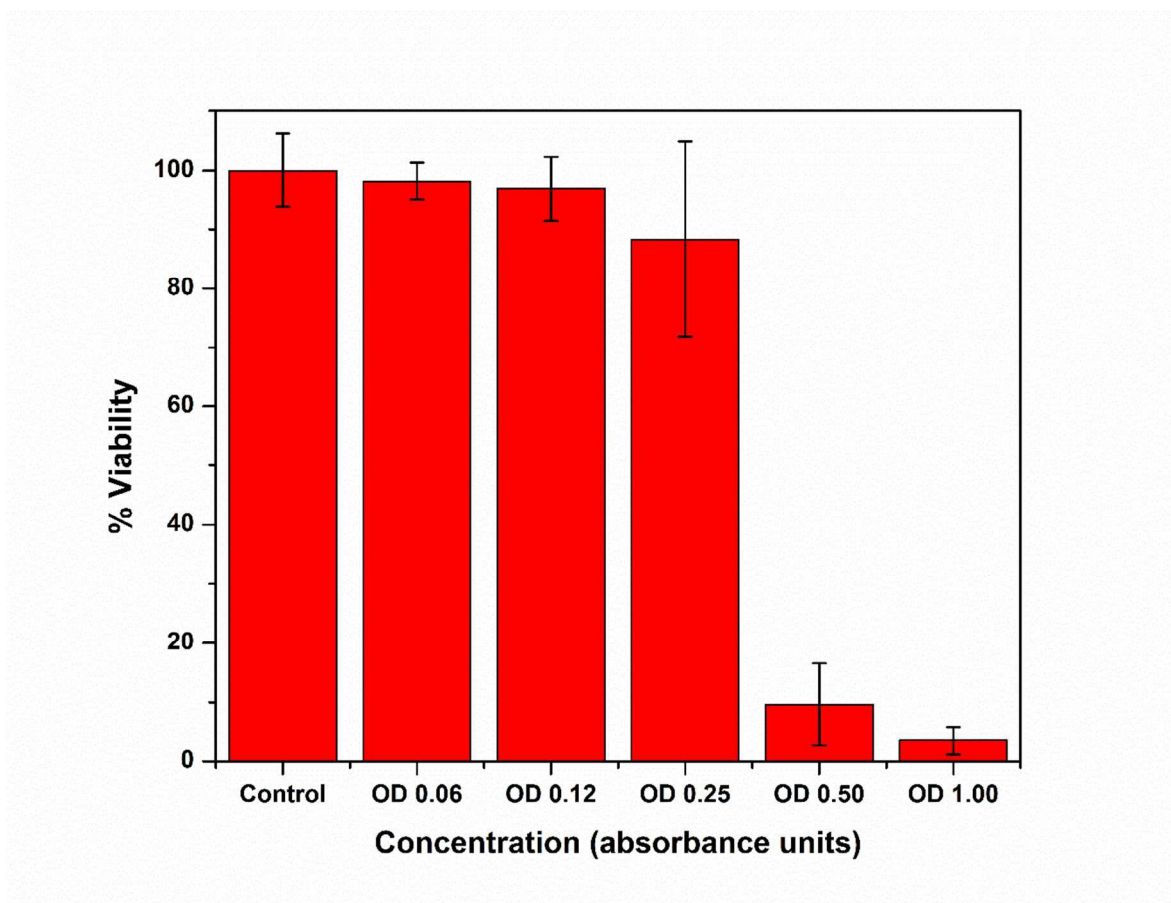
Figure 9. Cell viability of A549 cell line exposed to hollow nanoparticles at different concentrations as evaluated by MTT assay.

CONCLUSIONS

Hollow bimetallic Au-Ag nanoparticles were synthesized via a galvanic replacement reaction. The synthesized nanoparticles can be tuned to absorb light along the visible and near infrared region of the electromagnetic spectrum by a simple variation of the template size and the concentration of gold in solution. The pH and the use of the mild reducing agents affect the galvanic reaction mechanism and produce alloyed Au-Ag nanoparticles, which present good photothermal properties, reusability, and stability under long irradiation times with a NIR laser light. Taking into account their good optical properties and moderated cytotoxicity, these nanoparticles are good candidates for biomedical applications such as photothermal ablation therapy, photothermal nanoplatforms for drug delivery and similar other biomedical applications. These

nanoparticle systems could find their way and could be used effectively in several relevant advanced technological processes where plasmonic nanoheaters could be implemented.

REFERENCES

1   J. Z. Zhang, C. Noguez, *Plasmonics*, 2008, **3**, 127.

2   P. V. Kamat, *J. Phys. Chem. B*, 2002, **106**, 7729.

3   A. R. Lowery, A. M. Gobin, E. S. Day, N. J. Halas, J. L. West, *Int. J. Nanomed.*, 2006, **1**, 149.

4   P. K. Jain, X. Huang, I. H. El-Sayed, M. A. El-Sayed, *Acc. Chem. Res.*, 2008, **41**, 1578.

5   Y. Sun, Y. Xia, *Science*, 2002, **298**, 2176.

6   J. Chen, B. Wiley, Z.-Y. Li, D. Campbell, F. Saeki, H. Cang, L. Au, J. Lee, X. Li, Y. Xia, *Adv. Mater.*, 2005, **17**, 2255.

7   J. Z. Zhang, *J. Phys. Chem. Lett.*, 2010, **1**, 686.

8   N. Rozanova, J. Z. Zhang, *Sci. China Ser. B-Chem.*, 2009, **52**, 1559.

9   N. Halas, *Opt. Photonics News*, 2002, **13**, 26.

10 G. Fu, W. Liu, S. Feng, X. Yue, *Chem. Commun.*, 2012, **48**, 11567.

11 Q. Tian, J. Hu, Y. Zhu, R. Zou, Z. Chen, S. Yang, R. Li, Q. Su, Y. Han, X. Liu, *J. Am. Chem. Soc.*, 2013, **135**, 8571.

12 G. P. Luke, A. Bashyam, K. A. Homan, S. Makhija, Y. -S. Chen, S. Y. Emelianov, *Nanotechnology*, 2013, **24**, 455101.

13 J. Li, J. Han, T. Xu, C. Guo, X. Bu, H. Zhang, L. Wang, H. Sun, B. Yang, *Langmuir*, 2013, **29**, 7102.

14 Y. Qin, X. Ji, J. jing, H. Liu, H. Wu, W. Yang, *Colloids Surf., A*, 2010, **372**, 172.

15 G. Mie, *Ann. Phys.*, 1908, **25**, 377.

16 Y. Sun, Y. Xia, *Nano Lett.*, 2003, **3**, 1569.

17 X. Zou, E. Ying, S. Dong, *J. Colloid Interface Sci.*, 2007, **306**, 307.

18 Y. Sun, Y. Xia, *J. Am. Chem. Soc.*, 2004, **126**, 3892.

19 X. Xia, Y. Wang, A. Ruditskiy, Y. Xia, *Adv. Mater.*, 2013, **25**, 6313.

20 A. M. Schwartzberg, T. Y. Olson, C. E. Talley, J. Z. Zhang, *J. Phys. Chem. B*, 2006, **110**, 19935.

21 B. G. Prevo, S. A. Esakoff, A. Mikhailovsky, J. A. Zasadzinski, *Small*, 2008, **4**, 1183.

22 M. M. Shahjamali, M. Bosman, S. Cao, X. Huang, S. Saadat, E. Martinsson, D. Aili, Y. Y. Tay, B. Liedberg, S. C. J. Loo, H. Zhang, F. Boey, C. Xue, *Adv. Funct. Mater.*, 2012, **22**, 849.

23 R. G. Sanedrin, D. G. Georganopoulou, S. Park, C. A. Mirkin, *Adv. Mater.*, 2005, **17**, 1027.

24 Y. Yang, J. Liu, Z.-W. Fu, D. Qin, *J. Am. Chem. Soc.*, 2014, **136**, 8153.

25 L. Au, X. Lu, Y. Xia, *Adv. Mater.*, 2008, **20**, 2517.

26 H. Shi, L. Zhang, W. Cai, *J. Appl. Phys.*, 2000, **87**, 1572.

27 H.-N. Xie, I. A. Larmour, Y.-C. Chen, A. W. Wark, V. Tileli, D. W. McComb, K. Faulds, D. Graham, *Nanoscale*, 2013, **5**, 765.

28 Z. Liu, H. Song, L. Yu, L. Yang, *Appl. Phys. Lett.*, 2005, **86**, 113109.

29 Z. Liu, H. Song, L. Yu, L. Yang, G. Pan, *Sci. China Ser. B-Chem.*, 2005, **48**, 431.

30 C.-H. Li, A. C. Jamison, S. Rittikulsittichai, T.-C. Lee, T. R. Lee, *ACS Appl. Mater. Interfaces*, 2014, **6**, 19943.

31 D. K. Roper, W. Ahn, M. Hoepfner, *J. Chem. Phys. C*, 2007, **111**, 3636.

32 J. R. Cole, N. A. Mirin, M. W. Knight, G. P. Goodrich, N. J. Halas, *J. Phys. Chem. C*, 2009, **113**, 12090.

33 J. Zeng, D. Goldfeld, Y. Xia, *Angew. Chem. Int. Ed.*, 2013, **52**, 4169.

34 Z. Liu, L. Cheng, L. Zhang, Z. Yang, Z. Liu, J. Fang, *Biomaterials*, 2014, **35**, 4099.

35 L. M. Maestro, P. Haro-González, A. Sánchez-Iglesias, L. M. Liz-Marzán, J. García-Sole, D. Jaque, *Langmuir*, 2014, **30**, 1650.

36 D. A. Wheeler, R. J. Newhouse, H. Wang, S. Zou, J. Z. Zhang, *J. Phys. Chem. C*, 2010, **114**, 18126.

37 H. Wang, J. Han, W. Lu, J. Zhang, J. Li, L. Jiang, *J. Colloid Interface Sci.*, 2015, **440**, 236.

38 A. M. Alkilany, C. J. Murphy, *J. Nanopart. Res.*, 2010, **12**, 2313.

39 J. R. Lepock, *Int. J. Hyperthermia*, 2003, **19**, 252.
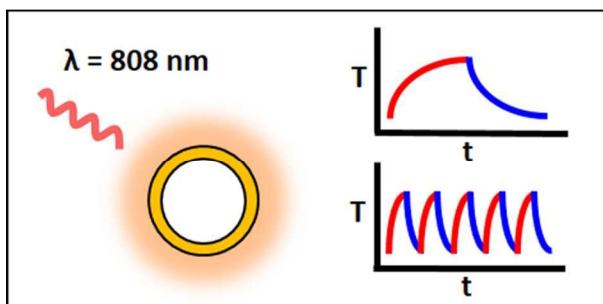
We report the synthesis of hollow Au-Ag bimetallic nanoparticles with **high photothermal stability** under NIR irradiation.